Preoperative Assessment of Pancreatic Cancer with FDG PET/MR Imaging versus FDG PET/CT Plus Contrast-enhanced Multidetector CT: A Prospective Preliminary Study[1]

Ijin Joo, MD
Jeong Min Lee, MD
Dong Ho Lee, MD
Eun Sun Lee, MD
Jin Chul Paeng, MD
Soo Jin Lee, MD
Jin-Young Jang, MD
Sun-Whe Kim, MD
Ji Kon Ryu, MD
Kyoung-Bun Lee, MD

Purpose: To determine the diagnostic performance of fluorine 18 fluorodeoxyglucose (FDG) positron emission tomography (PET)/magnetic resonance (MR) imaging in the preoperative assessment of pancreatic cancer in comparison with that of FDG PET/computed tomography (CT) plus contrast material–enhanced multidetector CT.

Materials and Methods: This prospective study was approved by the institutional review board; written informed consent was obtained. Thirty-seven patients with 39 pancreatic tumors underwent preoperative FDG PET/MR imaging, PET/CT, and contrast-enhanced multidetector CT. The authors measured maximal and mean standardized uptake values (SUV_{max} and SUV_{mean}, respectively) of pancreatic cancer at PET/MR imaging and PET/CT. Two radiologists independently reviewed the two imaging sets (set 1, PET/MR imaging; set 2, PET/CT plus multidetector CT) to determine tumor resectability according to a five-point scale, N stage (N0 or N positive), and M stage (M0 or M1). With use of clinical-surgical-pathologic findings as the standard of reference ($n = 20$), diagnostic performances of the two imaging sets were compared by using the McNemar test.

Results: Both SUV_{max} and SUV_{mean} of pancreatic tumors showed strong correlations between PET/MR imaging and PET/CT ($r = 0.897$ and 0.890, respectively; $P < .001$). The diagnostic performance of PET/MR imaging was not significantly different from that of PET/CT plus multidetector CT in the assessment of tumor resectability (area under the receiver operating characteristic curve: 0.891 vs 0.776, respectively, for reviewer 1 [$P = .109$] and 0.859 vs 0.797 for reviewer 2 [$P = .561$]), N stage (accuracy: 54% [seven of 13 patients] vs 31% [four of 13 patients]; $P = .250$ for both reviewers), and M stage (accuracy: 94% [16 of 17 patients] vs 88% [15 of 17 patients] for reviewer 1 [$P > .999$] and 94% [16 of 17 patients] vs 82% [14 of 17 patients] for reviewer 2 [$P = .500$]).

Conclusion: FDG PET/MR imaging showed a diagnostic performance similar to that of PET/CT plus contrast-enhanced multidetector CT in the preoperative evaluation of the resectability and staging of pancreatic tumors.

Online supplemental material is available for this article.

[1] From the Department of Radiology (I.J., J.M.L., D.H.L.), Institute of Radiation Medicine (J.M.L.), Department of Nuclear Medicine (J.C.P., S.J.L.), Department of Surgery and Cancer Research Institute (J.Y.J., S.W.K.), Division of Gastroenterology, Department of Internal Medicine (J.K.R.), and Department of Pathology (K.B.L.), Seoul National University Hospital, 101 Daehak-ro, Jongno-gu, Seoul 110-744, Korea; and Department of Radiology, Chung-Ang University Hospital, Seoul, Korea (E.S.L.). Received December 17, 2015; revision requested February 3, 2016; revision received May 1; accepted May 26; final version accepted June 3. **Address correspondence to** J.M.L. (e-mail: *jmsh@snu.ac.kr*).

Supported by National R&D Program for Cancer Control, Ministry of Health & Welfare, Republic of Korea (grant 1120310).

Pancreatic cancer is a highly lethal malignancy, with a 5-year survival rate of less than 5%, and is the fourth leading cause of cancer death in the United States and the eighth worldwide (1–4). In patients with this deadly cancer, assessment of the tumor's resectability, as well as accurate N staging and M staging, is of vital importance in the determination of the most appropriate treatment plan (eg, surgical resection, neoadjuvant treatment followed by surgery, or palliative treatment) and in the prediction of the patients' prognosis (5,6).

Contrast material–enhanced multidetector computed tomography (CT) is the most commonly used and best-validated imaging modality for the diagnosis and staging of pancreatic cancer (3,7). However, several studies have shown that contrast-enhanced magnetic resonance (MR) imaging with MR cholangiopancreatography can provide superior tumor conspicuity and similar diagnostic performance in evaluating the tumor resectability of pancreatic cancers compared with multidetector CT (8,9). Another modality that has shown potential is fluorine 18 fluorodeoxyglucose (FDG) positron emission tomography (PET)/CT, which has been reported to improve the detection of occult metastases when combined with contrast-enhanced CT in patients with locally resectable pancreatic cancer, ultimately sparing these patients from unnecessary surgery (10–12). Thus, at present, because of the different advantages of each imaging modality, multimodality imaging studies are being increasingly used in patients with pancreatic cancer at the cost of delayed surgical treatment for resectable diseases owing to this multistep process (3,7,13).

Recently, a whole-body integrated FDG PET/MR imaging system has become available for clinical use. This system has many potential advantages over PET/CT, including inherently lower radiation exposure, higher soft-tissue contrast, and multiparametric imaging capabilities (14). Indeed, several recent studies have demonstrated that PET/MR imaging can provide a diagnostic performance equivalent to or even better than that of PET/CT for the staging of various kinds of oncologic diseases in such organs as the liver and in bone, where MR imaging can provide distinct advantages over CT (15–20). For its use in pancreatic cancer, however, although a previous study has demonstrated the usefulness of PET/MR imaging in differential diagnosis (21), the preoperative role of PET/MR imaging for tumor staging and resectability of pancreatic tumors has not been reported. Thus, preliminary data on the differences in diagnostic performance between the two imaging systems would be useful for future power calculations in a main study comparing the performance of PET/MR imaging with that of the conventional combination of PET/CT plus multidetector CT.

Therefore, the purpose of this study was to compare the diagnostic performance of FDG PET/MR imaging in the preoperative assessment of pancreatic cancer with that of FDG PET/CT plus contrast-enhanced multidetector CT.

Advances in Knowledge

- In the preoperative prediction of the tumor resectability of pancreatic cancer, fluorine 18 fluorodeoxyglucose (FDG) PET/MR imaging was shown to be similar to PET/CT plus contrast material–enhanced multidetector CT (area under the receiver operating characteristic curve: 0.891 vs 0.776, respectively, for reviewer 1 [$P = .109$] and 0.859 vs 0.797 for reviewer 2 [$P = .561$]).
- The accuracy of FDG PET/MR imaging for preoperative N and M staging in patients with pancreatic cancer was similar to that of PET/CT plus multidetector CT (accuracy for N staging: 54% [seven of 13 patients] vs 31% [four of 13 patients] for both reviewers [$P = .250$]; accuracy of M staging: 94% [16 of 17 patients] vs 88% [15 of 17 patients] for reviewer 1 [$P > .999$] and 94% [16 of 17 patients] vs 82% [14 of 17 patients] for reviewer 2 [$P = .500$]).
- Standardized uptake values (SUVs) of pancreatic tumors measured at FDG PET/MR imaging and PET/CT showed very strong correlations (maximal SUV: $r = 0.897$, $P < .001$; mean SUV: $r = 0.890$, $P < .001$).

Implication for Patient Care

- FDG PET/MR imaging, as a one-step whole-body imaging tool, can potentially serve as an alternative to FDG PET/CT plus multidetector CT in the preoperative assessment of resectability and staging of pancreatic cancer, thereby shortening the work-up period for the determination of the therapeutic strategy.

Materials and Methods

This prospective preliminary study was supported by a grant from the National R&D Program for Cancer Control, Ministry of Health & Welfare, Republic of Korea (grant 1120310). This study was approved by the institutional review board, and written informed consent was obtained from all participants.

Published online before print
10.1148/radiol.2016152798 **Content code:** GI

Radiology 2017; 282:149–159

Abbreviations:
CI = confidence interval
DW = diffusion weighted
FDG = fluorine 18 fluorodeoxyglucose
SUV = standardized uptake value
SUV_{max} = maximal SUV
SUV_{mean} = mean SUV

Author contributions:
Guarantors of integrity of entire study, I.J., J.M.L., J.Y.J., J.K.R.; study concepts/study design or data acquisition or data analysis/interpretation, all authors; manuscript drafting or manuscript revision for important intellectual content, all authors; manuscript final version approval, all authors; agrees to ensure any questions related to the work are appropriately resolved, all authors; literature research, I.J., J.M.L.; clinical studies, all authors; statistical analysis, I.J.; and manuscript editing, I.J., J.M.L., D.H.L., J.C.P.

Conflicts of interest are listed at the end of this article.

Figure 1

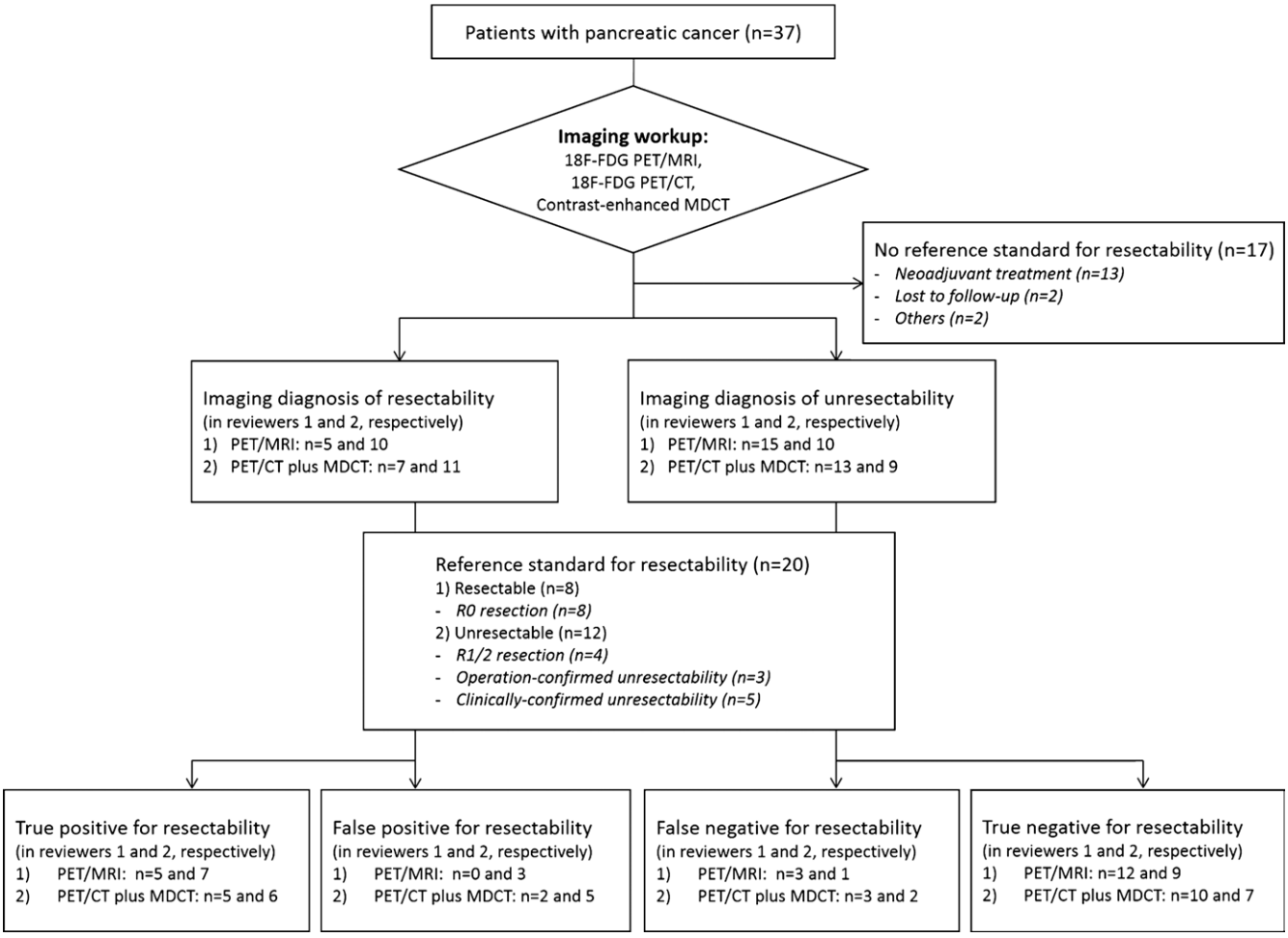

Figure 1: Flow diagram of the study population. *MDCT* = multidetector CT.

Patients

From February 2013 to April 2014, 37 consecutive patients (20 men and 17 women; mean age ± standard deviation, 62.8 years ± 9.9) scheduled to undergo surgery for pancreatic cancer confirmed at histopathologic examination or suspected on the basis of multidetector CT findings were enrolled in this study. Among these 37 patients, 35 patients were initially diagnosed as having pancreatic cancer, one patient had developed pancreatic cancer in the remnant pancreas after resection, and one patient had completed preoperative concurrent chemotherapy and radiation therapy for the known pancreatic cancer. Of note, our study population included 28 patients who had also been enrolled in a prospective randomized phase II/III study titled "Neoadjuvant Chemoradiation in Patients with Borderline Resectable Pancreatic Cancer Study" (NCT01458717). All patients underwent FDG PET/MR imaging, FDG PET/CT, and contrast-enhanced multidetector CT within 2 weeks (Fig 1).

Image Acquisition

Before PET/MR imaging or PET/CT, each patient was asked to fast for at least 6 hours. Then, serum glucose levels were checked to ensure they were less than 200 mg/dL and each patient received an intravenous injection of FDG (5.2 MBq per kilogram body weight). Between 50 and 90 minutes after the administration of FDG, acquisitions of PET/MR imaging or PET/CT were started. In patients undergoing same-day PET/MR imaging and PET/CT (n = 33), the two imaging studies (PET/CT first, followed by PET/MR imaging) were performed sequentially with an interval of less than 30 minutes after a single injection of the tracer. Conversely, in patients who underwent PET/MR imaging and PET/CT on different days (n = 4), each study was performed after injection of the tracer on the study day.

PET/MR imaging protocol.—All FDG PET/MR imaging studies were performed with a combined whole-body

system (Biograph mMR; Siemens Healthcare, Erlangen, Germany) based on a 3.0-T MR imager capable of simultaneous acquisition of PET and MR images. Our PET/MR imaging protocol included two parts: *(a)* whole-body PET/MR imaging and *(b)* dedicated pancreatic MR imaging with MR cholangiopancreatography. Whole-body PET was performed from the brain to the midthigh, encompassing five bed positions (each bed position had an acquisition time of approximately 3 minutes, coverage of 25.8 cm in length, and 6.1-cm overlap between adjacent positions). Simultaneous MR imaging was conducted per bed, including Dixon-based coronal two-point volumetric interpolated breath-hold examination for automatic correction of the PET attenuation and transverse half-Fourier acquisition single-shot turbo spin-echo imaging. In addition, dedicated pancreatic MR imaging with MR cholangiopancreatography (included sequences are in Table E1 [online]) was performed with coverage from the liver dome to the third portion of the duodenum. The overall imaging time for PET/MR imaging was approximately 60 minutes for each patient.

PET/CT protocol.—FDG PET/CT studies were performed with one of two integrated scanners at our institution (Biograph mCT 64 or mCT 40, Siemens Healthcare; $n = 34$ and $n = 2$, respectively) or one integrated scanner at an outside hospital (Discovery 600, GE Healthcare, Chicago, Ill; $n = 1$). At our institution, CT images were obtained from the skull base to the midthigh by using 40 mAs and 120 kVp (adjusted for body thickness) and reconstructed into image matrices of 512 × 512 for attenuation correction. No iodinated contrast material was used. After CT images were obtained, whole-body PET was performed, encompassing seven to nine bed positions (each bed position had an acquisition time of approximately 1 minute and a coverage of 21.6 cm in length). PET images were reconstructed into image matrices of 200 × 200 iteratively by using ordered subset expectation maximization (two iterations, 21 subsets). The overall imaging time for PET/CT was approximately 10 minutes for each patient.

Contrast-enhanced multidetector CT.—CT images were obtained by using several kinds of multidetector CT scanners: one 320-channel scanner (Aquilion ONE, Toshiba Medical Systems, Tustin, Calif; n = 23), one 128-channel scanner (Ingenuity, Philips Healthcare, Amsterdam, the Netherlands; n = 6), two 64-channel scanners (Brilliance 64, Philips Medical Systems [n = 2], and Somatom Definition, Siemens Healthcare [n = 3]), and one 16-channel scanner (Sensation 16, Siemens Healthcare; n = 1) at our institution and 64-channel scanners at the outside hospital (n = 2). Imaging parameters for the multidetector CT scanners at our institution are summarized in Table E2 (online).

Measurement of Maximal and Mean Standardized Uptake Values in Pancreatic Tumors

Standardized uptake values (SUVs) were measured at PET/MR imaging and PET/CT by one nuclear medicine physician (S.J.L., with 4 years of experience in PET/CT imaging), who was provided information about the number and location of the pancreatic tumors for each patient. An isoactivity-contoured volume of interest encircling the pancreatic tumor was drawn under the guidance of corresponding MR or CT images by setting the margin threshold as 50% of maximal uptake. In this volume of interest, the maximal SUV (SUV_{max}) and mean SUV (SUV_{mean}) of pancreatic tumors were measured.

Image Interpretation

All images were retrospectively reviewed in two sessions by two independent abdominal radiologists (D.H.L. and E.S.L., with 10 and 9 years of experience in abdominal CT and MR imaging and with 3 years of experience in PET/MR imaging) who were blinded to the clinical-surgical-pathologic results except for the information that all patients were confirmed to have pancreatic cancer. In each session, one of two image sets (set 1, PET/MR imaging; set 2, PET/CT plus contrast-enhanced multidetector CT) was reviewed. One radiologist reviewed image set 1 followed by set 2 and the other radiologist reviewed image set 2 followed by set 1. Image sets were read after an interval of 4 weeks and a reshuffling of the image review order to minimize recall bias.

Assessment of tumor conspicuity.—With regard to the conspicuity of pancreatic tumors, the reviewers were asked to assign a confidence level on the basis of a five-point scale, as follows: 5, there was a clear tumor margin showing at least 90% of the tumor circumference; 4, there was a clear tumor margin showing 50%–90% of the tumor circumference; 3, there was a clear tumor margin showing 10%–50% of the tumor circumference; 2, there was a clear tumor margin showing less than 10% of the tumor circumference; and 1, no visible tumor (22).

Assessment of tumor resectability.—The reviewers were also asked to determine the resectability of pancreatic tumors on the basis of local tumor extent and the presence or absence of distant metastasis by using a five-point scale, as follows: 5, definitely resectable; 4, probably resectable; 3, indeterminate probability for resectability; 2, probably unresectable; and 1, definitely unresectable (Appendix E1 [online]) (23). If a patient had more than one suspected pancreatic tumor, the per-patient tumor resectability was determined by using the lower scored lesion.

Determination of N stage.—At imaging assessment of per-patient N stage, positive lymph nodes were determined on the basis of their size, visual assessment of PET images, and/or diffusion restriction. If the largest regional lymph node was at least 8 mm in its shortest diameter and/or positive at visual assessment of PET scans, the patient would be considered as node positive; otherwise, patients were considered node negative. In addition, at PET/MR imaging, if any lymph nodes had higher signal intensity than muscle at diffusion-weighted (DW) imaging according to *b* values of 400 or 800 sec/mm^2, the patient would be classified as node positive (24–26).

Determination of M stage.—At imaging assessment of per-patient M stage, M1 stage was assigned if there were lesions with a high suspicion for

distant metastases. At PET/MR imaging, the presence of distant metastases was determined on the basis of routine MR sequences, high signal intensity at DW imaging with *b* values of 400 or 800 sec/mm^2, and positivity on PET scans at visual assessment. On the PET/CT plus multidetector CT set, positivity on multidetector CT and/or PET scans was used for the determination of M stage for each patient.

Clinical-Surgical-Pathologic Findings

The standard of reference for tumor resectability was based on surgical records, results of pathologic examination, and imaging-based decisions. In patients who underwent surgery within 4 weeks after preoperative imaging, tumor resectability was assessed according to surgical records and pathology reports, as follows: R0 (no residual tumor) resection was defined as resectable, and R1 (microscopic residual tumor) resection, R2 (macroscopic residual tumor) resection, no resection of the pancreatic mass owing to unresectability confirmed during surgery, and presence of pathologically confirmed distant metastasis were defined as unresectable. In addition, if a patient had distant metastases and/or locally unresectable cancer at preoperative imaging and did not undergo surgery on the basis of a multidisciplinary conference, he or she was regarded as having clinically confirmed unresectable disease. The standard of reference for N staging was determined by the pathologic findings in patients who underwent regional lymph node dissection. For M staging, the standard of reference of M0 was determined with histopathologic results, whereas that of M1 was determined with histopathologic evaluation or imaging-based decisions made by means of a multidisciplinary conference.

Statistical Analysis

SUVs (SUV_{max} and SUV_{mean}) of pancreatic tumors were compared on a per-lesion basis between PET/MR imaging and PET/CT by using the paired *t* test assuming equal variances. Because the raw data from one PET/CT examination were not available (that examination was performed at an outside hospital), SUVs for PET/CT were measured in 38 pancreatic tumors in 36 patients; those for PET/MR imaging were measured in 39 tumors in 37 patients. Therefore, per-lesion–based comparison of SUVs was performed for only 38 lesions. The correlation between SUVs with PET/MR imaging and PET/CT was evaluated by using Pearson correlation coefficient analysis. The Pearson *r* was interpreted as follows: poor correlation, less than 0.20; weak correlation, 0.20–0.39; moderate correlation, 0.40–0.59; strong correlation, 0.6–0.8; and very strong correlation, 0.80 or greater. Per-lesion tumor conspicuity (n = 39) on the PET/MR imaging set and on the PET/CT plus multidetector CT set was compared by using the paired *t* test. Interobserver agreements on per-patient tumor resectability, N stage, and M stage (n = 37) were analyzed by using κ statistics and interpreted as follows: poor, less than 0.20; fair, 0.20–0.39; moderate, 0.40–0.59; substantial, 0.60–0.79; and almost perfect, 0.80 or greater.

Diagnostic performances of each reviewer for per-patient resectability, N staging, and M staging were evaluated in patients by using standards of reference. Tumor resectability was evaluated with empirical receiver operating characteristic curve analysis on the basis of a five-point confidence scale. The area under the receiver operating characteristic curve was considered indicative of diagnostic performance, and areas under the receiver operating characteristic curve values of the two imaging sets were compared by using the z test. In addition, for examinations given scores of 4 or 5 (probably or definitely resectable), indicating an imaging diagnosis of resectable, the sensitivity, specificity, and accuracy of the imaging diagnosis were calculated. For tumor resectability, N stage, M stage, sensitivity, specificity, and accuracy were compared between PET/MR imaging and PET/CT plus multidetector CT by using the McNemar test. All statistical analyses were performed with a commercially available software package (MedCalc, version 15.8; MedCalc Software, Mariakerke, Belgium). Two-tailed $P < .05$ was considered to indicate a statistically significant difference.

Results

Clinical-Surgical-Pathologic Findings

Thirty-nine pancreatic tumors (two tumors each were found in two patients; one tumor was found in 35 patients) were finally confirmed with histopathologic evaluation by upfront or delayed surgical resection or endoscopic ultrasonographically guided biopsy. Among the 37 patients, per-patient tumor resectability was confirmed in 20 patients (resectable, n = 8; unresectable, n = 12). Tumor resectability could not be confirmed in 17 patients: Thirteen patients had undergone neoadjuvant concurrent chemotherapy and radiation therapy or chemotherapy, two patients were lost to follow-up, and two patients had their surgeries canceled because of incidentally found lung cancer or acute pancreatitis (Fig 1).

N stage was confirmed with histopathologic findings in 13 patients (node negative, n = 3; node positive, n = 10) who underwent surgical resection for pancreatic cancer, and M stage was confirmed in 17 patients (M0, n = 13; M1, n = 4) by means of histopathologic reports (M0, n = 13; M1, n = 2) or imaging-based diagnosis (M1, n = 2). For M stage, three patients who did not undergo surgery because locally unresectable disease was diagnosed clinically were not included in the analysis (they lacked a standard of reference for distant metastases). The M1 stage results include one patient with peritoneal seeding found during surgery, one patient with hepatic metastases confirmed with laparoscopic biopsy, one patient with an imaging-based diagnosis of hepatic metastases, and one patient with an imaging-based diagnosis of distant lymph node metastasis.

SUVs of Pancreatic Cancer: PET/MR Imaging versus PET/CT

The per-lesion pairwise comparison of SUVs at PET/MR imaging and PET/CT showed that both the SUV_{max} and SUV_{mean} of pancreatic tumors (n = 38)

at PET/MR imaging were significantly lower than those at PET/CT ($P < .001$) (Table 1). However, those values showed very strong correlations between PET/MR imaging and PET/CT, with correlation coefficients of 0.897 for SUV_{max} and 0.890 for SUV_{mean} ($P < .001$) (Fig 2).

Conspicuity of Pancreatic Tumors: PET/MR Imaging versus PET/CT Plus Multidetector CT

All 39 pancreatic tumors were detected on both imaging sets and received a tumor conspicuity score of 2 or greater by both reviewers. For both reviewers, tumor conspicuity was slightly better at PET/MR imaging than at PET/CT; however, there was no statistically significant difference (score: 3.49 ± 0.79 vs 3.23 ± 0.74, respectively, for reviewer 1 [$P = .096$] and 3.64 ± 0.99 vs 3.36 ± 1.01 for reviewer 2 [$P = .094$]) (Fig 3).

Assessment of Tumor Resectability and N and M Staging: PET/MR Imaging versus PET/CT Plus Multidetector CT

Interobserver agreement.—In the 37 patients in our study population, the PET/MR imaging set showed moderate interobserver agreement with regard to tumor resectability (weighted κ = 0.459; 95% CI: 0.268, 0.651) and substantial agreement with regard to N stage (κ = 0.682; 95% CI: 0.461, 0.903) and M stage (κ = 0.611; 95% CI: 0.279, 0.943). The PET/CT plus multidetector CT set showed moderate interobserver agreement with regard to tumor resectability (weighted κ = 0.413; 95% CI: 0.210, 0.615), N stage (κ = 0.554; 95% CI: 0.368, 0.879), and M stage (κ = 0.528; 95% CI: 0.060, 0.995).

Tumor resectability (n = 20).—For the evaluation of per-patient tumor resectability, there were no significant differences in the areas under the receiver operating characteristic curve between the PET/MR imaging set and the PET/CT plus multidetector CT set (0.891 vs 0.776 for reviewer 1 [$P = .109$] and 0.859 vs 0.797 for reviewer 2 [$P = .561$]) (Table 2, Fig 2). When scores of 4 and 5 (ie, probably or definitely resectable) were categorized as indicating an imaging diagnosis of tumor resectability, the PET/MR imaging set and PET/CT plus multidetector CT set showed accuracies of 85% (17 of 20 patients) versus 75% (15 of 20 patients), respectively, for reviewer 1 and 80% (16 of 20 patients) versus 65% (13 of 20 patients) for reviewer 2, without a significant difference between imaging sets ($P = .500$ and .375, respectively) (Table 2).

N staging (n = 13).—Diagnostic accuracies were not significantly different between the two image sets for both reviewers (54% [seven of 13 patients] with PET/MR imaging vs 31% [four of 13 patients] with PET/CT plus multidetector CT; $P = .250$) (Table 3).

Table 1

SUVs of Pancreatic Tumors at PET/MR Imaging and PET/CT

Parameter and Imaging Modality	SUV*	Correlation Coefficient†
SUV_{max}		0.897
PET/MR imaging	7.15 ± 4.09 (2.35–21.77)	
PET/CT	11.89 ± 6.69 (4.79–37.27)	
P value	<.001	
SUV_{mean}		0.890
PET/MR imaging	4.80 ± 2.90 (1.68–15.28)	
PET/CT	7.88 ± 4.66 (2.85–25.91)	
P value	<.001	

* Calculated with the paired *t* test. Data are means ± standard deviations, with ranges in parentheses.

† Calculated with Pearson correlation coefficient analysis.

Figure 2

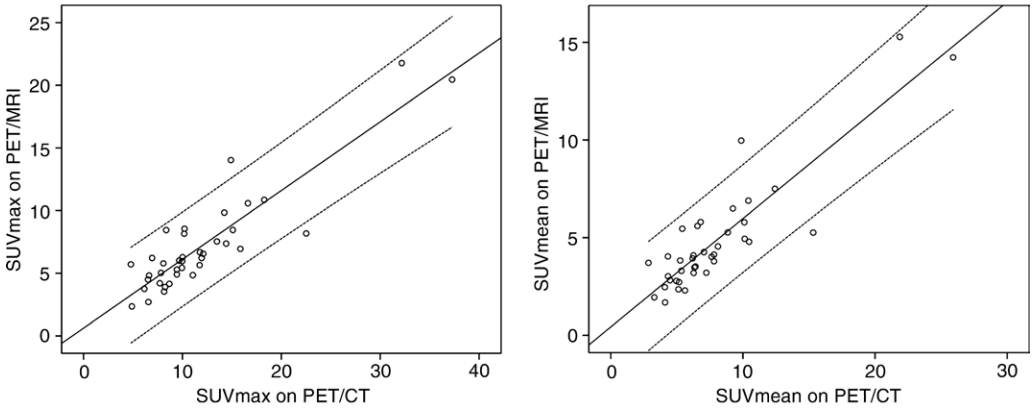

Figure 2: Graphs show correlations of **(a)** SUV_{max} and **(b)** SUV_{mean} of pancreatic cancers between FDG PET/MR imaging and FDG PET/CT. Solid and dotted lines represent linear regression line and 95% confidence interval (CI), respectively.

In the depiction of any regional lymph node metastasis per patient, PET/MR imaging showed higher sensitivity than PET/CT plus multidetector CT (40% [four of 10 patients] vs 10% [one of 10 patients], respectively, for both reviewers), although there were no statistically significant differences (P = .250) (Fig 4). In addition, both imaging sets showed high specificity (100% [three of three patients]) for N staging for both reviewers.

M staging (n = 17).—For M staging, the PET/MR imaging set and PET/CT plus multidetector CT set demonstrated sensitivities of 75% (three of four patients) and 50% (two of four patients), respectively, for both reviewers, without a statistically significant difference (Table 3). Missed diagnoses of distant metastases occurred in one patient with peritoneal seeding that was missed by both reviewers on both imaging sets and one patient with liver metastases identified at PET/MR imaging but missed at PET/CT plus multidetector CT by both reviewers (Fig 5).

Discussion

In this prospective study, we demonstrated that FDG PET/MR imaging showed similar diagnostic performance without a statistically significant difference in the assessment of the tumor resectability, N stage, and M stage of pancreatic tumors compared with the widely used combination of FDG PET/CT plus contrast-enhanced multidetector CT. In addition, the SUV_{max} and SUV_{mean} of pancreatic cancers showed strong correlations between PET/MR imaging and PET/CT. Although this study is only exploratory, with a small number of patients, the findings suggest that PET/MR imaging, as a "one-stop-shop" examination, may be a potential alternative tool for the preoperative evaluation of pancreatic cancer, leading to improvement in creating a more efficient work-up flow. Indeed, according to a recent study (27), the negative predictive value of multidetector CT in the preoperative diagnosis of distant metastatic disease in patients with pancreatic cancer significantly decreased after 4 weeks because the tumor can metastasize during the interval between multidetector CT and surgery. Therefore, PET/MR imaging may play a valuable role by shortening the work-up period of suspected pancreatic tumors, avoiding conversion from resectable status to unresectable status because of the aggressive biologic character of pancreatic tumors.

In patients with pancreatic cancer, achievement of a margin-negative resection is the main treatment goal; thus, preoperative assessment of tumor resectability is crucial (28). In our study, the diagnostic performance of PET/MR

Figure 3

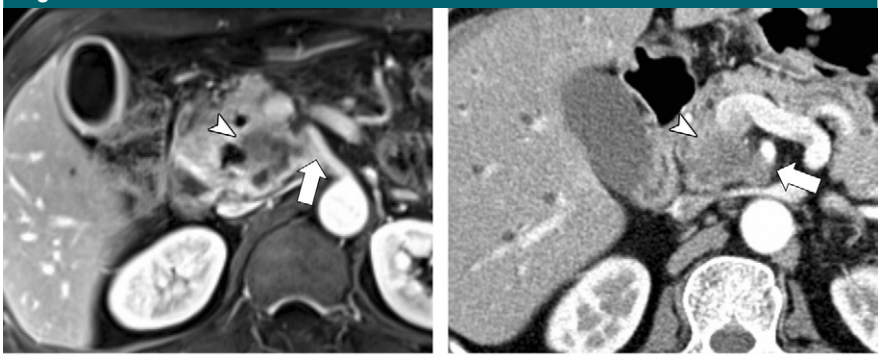

a. b.

Figure 3: Images of pancreatic ductal adenocarcinoma in 62-year-old man. **(a)** Venous phase PET/MR image shows hypointense mass in uncinate process of pancreas abutting superior mesenteric artery (arrow). **(b)** Pancreatic phase multidetector CT image shows mass abutting superior mesenteric artery (arrow). This patient underwent R1 resection because of tumor invasion of superior mesenteric artery. Note that tumor conspicuity is higher at MR imaging (**a**) than multidetector CT (**b**) (arrowhead).

Table 2

Diagnostic Performance of PET/MR Imaging and PET/CT Plus Multidetector CT in the Assessment of Tumor Resectability

Reviewer and Modality	A_z*	Sensitivity (%)†	Specificity (%)†	Accuracy (%)†
Reviewer 1				
PET/MR imaging	0.891 (0.671, 0.984)	62 (5/8)	100 (12/12)	85 (17/20)
PET/CT + MDCT	0.776 (0.537, 0.929)	62 (5/8)	83 (10/12)	75 (15/20)
P value	.109	NA	.500	.500
Reviewer 2				
PET/MR imaging	0.859 (0.632, 0.972)	87 (7/8)	75 (9/12)	80 (16/20)
PET/CT + MDCT	0.797 (0.560, 0.941)	75 (6/8)	58 (7/12)	65 (13/20)
P value	.561	>.999	.625	.375

Note.—MDCT = multidetector CT, NA = not assessable.

* A_z = area under the receiver operating characteristic curve. Data were calculated with the z test. Numbers in parentheses are 95% CIs.

† Calculated with the McNemar test. Numbers in parentheses are numbers of patients.

Table 3

Diagnostic Performances of PET/MR Imaging and PET/CT Plus Multidetector CT in the Assessment of N and M Stage

Reviewer and Modality	N Staging (%)			M Staging (%)		
	Sensitivity	Specificity	Accuracy	Sensitivity	Specificity	Accuracy
Reviewer 1						
PET/MR imaging	40.0 (4/10)	100 (3/3)	54 (7/13)	75 (3/4)	100 (13/13)	94 (16/17)
PET/CT + MDCT	10.0 (1/10)	100 (3/3)	31 (4/13)	50 (2/4)	100 (13/13)	88 (15/17)
P value	.250	NA	.250	>.999	NA	>.999
Reviewer 2						
PET/MR imaging	40.0 (4/10)	100 (3/3)	54 (7/13)	75 (3/4)	100 (13/13)	94 (16/17)
PET/CT + MDCT	10.0 (1/10)	100 (3/3)	31 (4/13)	50 (3/4)	92 (12/13)	82 (14/17)
P value	.250	NA	.250	>.999	>.999	.500

Note.—*P* values were calculated by using the McNemar test. Data in parentheses are numbers of patients used to calculate percentages. MDCT = multidetector CT, NA = not assessable

Figure 4

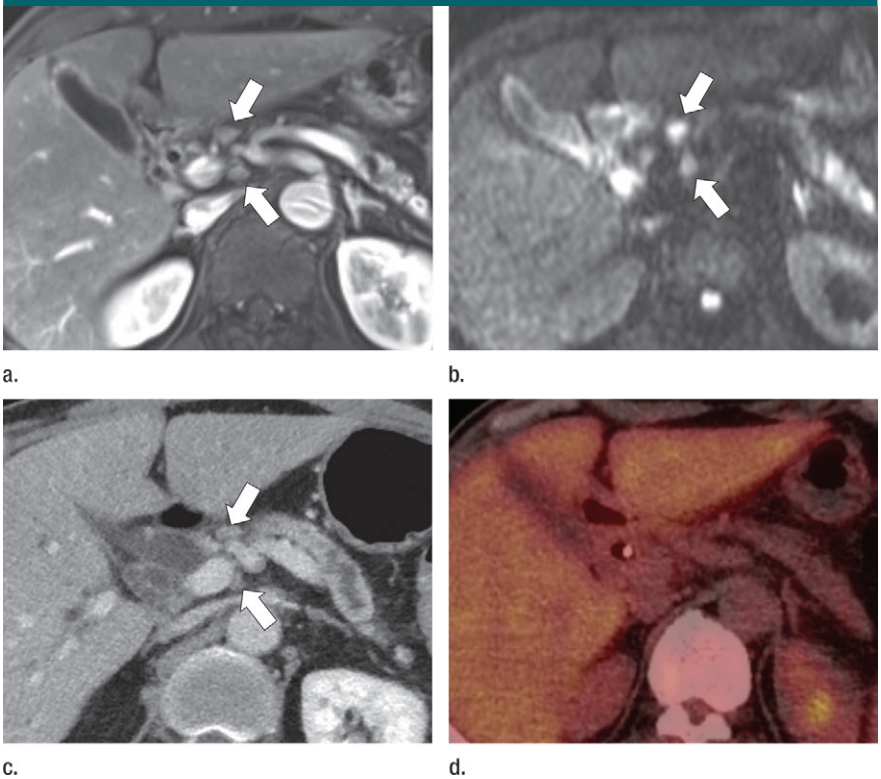

Figure 4: Images of histopathologically confirmed pancreatic cancer in 58-year-old man. **(a)** Venous phase MR image shows several small lymph nodes (arrows) along common hepatic artery. **(b)** DW image (b = 800 sec/mm^2) shows lymph nodes with restricted diffusion (arrows). Both reviewers interpreted this patient as being node positive on PET/MR imaging set. **(c)** Multidetector CT scan shows that these lymph nodes (arrows) are small, with a short diameter of less than 8 mm. **(d)** PET/CT scan shows that lymph nodes do not show hypermetabolism. Therefore, this patient's findings were interpreted as node negative on PET/CT plus multidetector CT set. Histopathologic results revealed this patient to be node positive.

imaging in terms of tumor resectability was comparable with that of PET/CT plus multidetector CT. These results are in good agreement with those of previous studies and can be explained by the similar individual performance of MR imaging and multidetector CT in the evaluation of the presence and/or extent of vascular involvement of pancreatic tumors (8). Considering that our study population included many patients with borderline resectable pancreatic tumors, our study performance may actually have been underestimated. However, because borderline resectable pancreatic tumors are a challenging problem in terms of determining resectability, our results showing a similar performance between PET/MR imaging and PET/CT plus multidetector CT would be meaningful. In addition, the tumor conspicuity on imaging studies is also important for the differential diagnosis between pancreatic cancer and benign strictures of the pancreatic duct, as well as in the detection of pancreatic cancers at its early stage, which can lead to curative resection and a better prognosis (29). Although our preliminary study failed to demonstrate a significant difference between PET/MR imaging and multidetector CT plus PET/CT in the assessment of the conspicuity of pancreatic tumors, previous studies have demonstrated that the addition of DW imaging to MR imaging improves the assessment of pancreatic tumor conspicuity compared with multidetector CT (8,22).

Precise assessment of lymph node metastases in patients with pancreatic cancer is an important factor in the accurate prediction of a patient's prognosis (30). Thus, PET/MR imaging, which provides anatomic information, as well as PET and DW imaging, can be useful in the detection and characterization of lymph nodes. However, in our study, which used imaging criteria such as size, PET positivity, and DW imaging positivity for N staging, both imaging sets showed low sensitivities, albeit with high specificities. Size-based assessment of lymph nodes has a limitation because reactive lymph nodes can be enlarged and small lymph nodes can

Figure 5

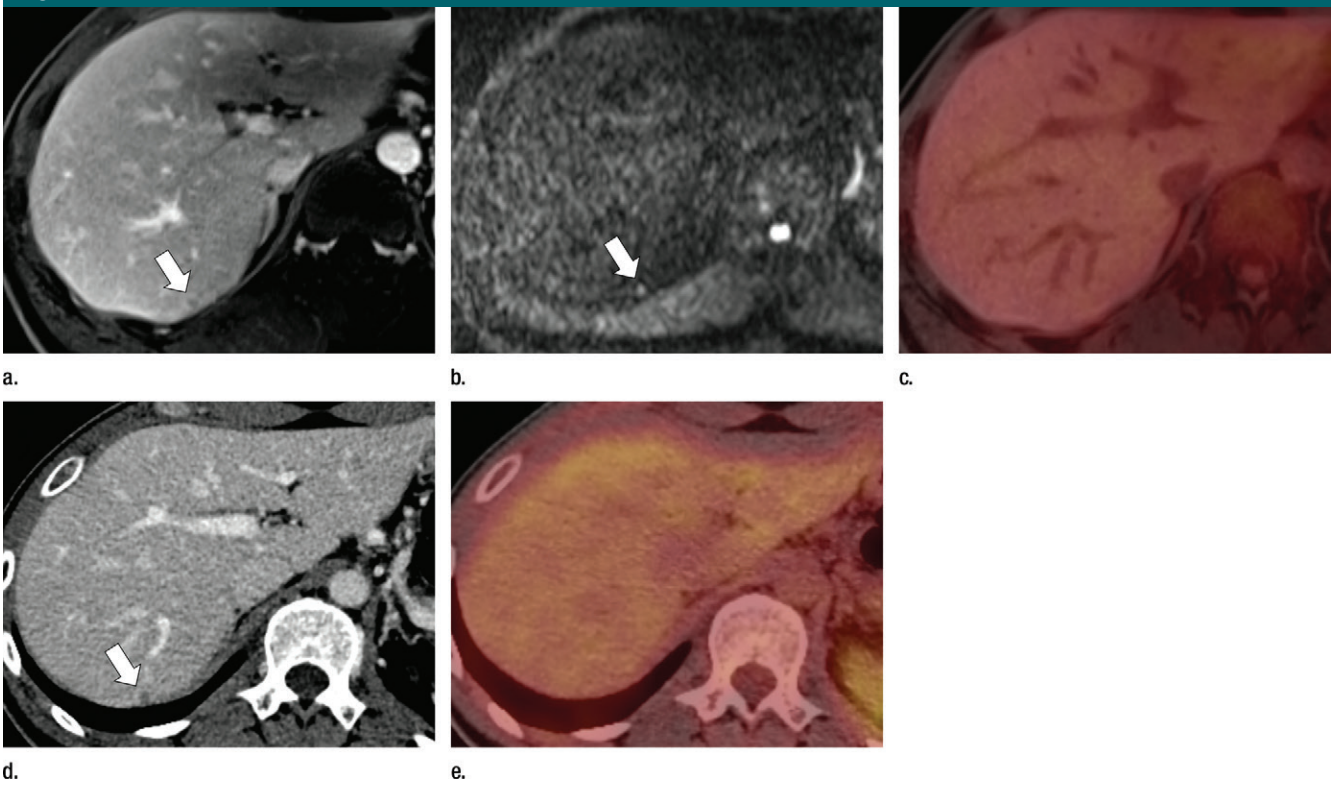

Figure 5: Histopathologically confirmed pancreatic cancer in 28-year-old man. **(a)** Venous phase MR image shows a small hypointense nodular lesion in segment VII of liver (arrow). **(b)** DW image (b = 800 sec/mm^2) shows nodule with restricted diffusion (arrow). **(c)** Corresponding PET/MR imaging fusion image shows nodule does not show hypermetabolism. **(d)** Venous phase multidetector CT image shows nodule as a hypoattenuating lesion (arrow). **(e)** PET/CT fusion image shows that there was no hypermetabolic lesion in liver. Both reviewers interpreted this patient as having stage M1 disease on PET/MR imaging set but stage M0 disease on PET/CT plus multidetector CT set. This patient was confirmed as having stage M1 disease at laparoscopic biopsy of hepatic surface nodule.

have micrometastases (31). In addition, PET has been reported to show limited performance in the detection of lymph node metastases, especially in small lesions (32). With the addition of DW imaging information, however, PET/MR imaging may increase the sensitivity for lymph node metastases, as shown in our study (40.0% [four of 10 patients] with PET/MR imaging vs 10.0% [one of 10 patients] with PET/CT plus multidetector CT). This additional role of DW imaging in N staging has also been reported for other malignancies (25,31).

As for M staging, diagnostic performance did not significantly differ between PET/MR imaging and PET/CT plus multidetector CT in our study. However, when we consider the results of previous studies that suggested that MR imaging with DW imaging would be superior to contrast-enhanced multidetector CT in the detection of metastases in the liver (the most common site of distant metastasis from pancreatic cancer [33,34]), and that the PET imaging performance of PET/MR imaging would be similar to that of PET/CT (20,35,36), future studies with a larger population are warranted. Furthermore, because both PET/MR imaging and PET/CT have shown limited performance in the detection of lung metastases, CT of the chest may be additionally required in the preoperative work-up of pancreatic tumors (20).

Finally, our results revealed strong correlations between SUVs of pancreatic tumors at PET/MR imaging and PET/CT, although PET/MR imaging resulted in underestimated SUVs in comparison with PET/CT. This result is in good agreement with findings of previous studies on various lesions as well as normal structures (37,38). The differences in SUVs between PET/MR imaging and PET/CT can be mainly attributed to the differences in MR imaging–based and CT-based attenuation correction techniques (20). Yet, although most of our study population underwent PET/CT immediately followed by PET/MR imaging, changes in SUV with time between the two imaging studies could not be completely avoided; such changes may have affected the lower SUV at PET/MR imaging compared with PET/CT. Because the major role of PET imaging in the initial staging would be in the detection of small distant metastases, PET/MR imaging may be used as an alternative to PET/CT in patients with pancreatic

tumors in the aspect of PET imaging. However, considering the significant difference in measured SUVs between the two modalities, for the purposes of quantification (which would be particularly important in the assessment of tumor response), longitudinal monitoring should be performed with a single modality of PET/MR imaging or PET/CT.

This study had several limitations. First, a relatively small number of patients were enrolled in this prospective study and reference standards for resectability and staging were determined only in a portion of patients—mainly because some patients with borderline-resectable pancreatic cancers were assigned to undergo neoadjuvant treatment after preoperative imaging work-up. Second, we assessed per-patient resectability and the staging of pancreatic tumors but did not compare imaging features and pathologic findings on a lesion-by-lesion basis. Thus, we could not match the imaging-based diagnosis of vascular involvement and/or lymph node status with the corresponding pathologic diagnoses. Third, we did not evaluate whether functional parameters of PET/MR imaging, such as SUV and apparent diffusion coefficient, could be used as surrogate markers for the evaluation of tumor response or the prediction of patients' prognoses because of the small number of patients receiving heterogeneous management in this preliminary study and the limited follow-up period. Therefore, further studies dealing with more patients and using serial assessment of tumor response and/or long-term follow-up would be needed to identify the additional value of PET/MR imaging.

In conclusion, FDG PET/MR imaging showed comparable diagnostic performance to PET/CT plus contrast-enhanced multidetector CT in the preoperative evaluation of the resectability and staging of pancreatic cancers.

Acknowledgment: We thank Chris Woo, BA, for his assistance in editing the manuscript.

Disclosures of Conflicts of Interest: I.J. disclosed no relevant relationships. **J.M.L.** Activities related to the present article: disclosed no relevant relationships. Activities not related to the present article: is a paid consultant for Siemens Healthcare; received grants from Donseo Medical, CMS, Acuzen, Starmed, RF Medical, Bayer Healthcare, Guerbet, and Samsung Medison; received honorarium from Bayer Healthcare and Guerbet. Other relationships: disclosed no relevant relationships. **D.H.L.** disclosed no relevant relationships. **E.S.L.** disclosed no relevant relationships. **J.C.P.** disclosed no relevant relationships. **S.J.L.** disclosed no relevant relationships. **J.Y.J.** disclosed no relevant relationships. **S.W.K.** disclosed no relevant relationships. **J.K.R.** disclosed no relevant relationships. **K.B.L.** disclosed no relevant relationships.

References

1. Abulkhir A, Limongelli P, Healey AJ, et al. Preoperative portal vein embolization for major liver resection: a meta-analysis. Ann Surg 2008;247(1):49–57.
2. Jemal A, Bray F, Center MM, Ferlay J, Ward E, Forman D. Global cancer statistics. CA Cancer J Clin 2011;61(2):69–90.
3. Pietryga JA, Morgan DE. Imaging preoperatively for pancreatic adenocarcinoma. J Gastrointest Oncol 2015;6(4):343–357.
4. Saif MW. Advancements in the management of pancreatic cancer: 2013. JOP 2013;14(2):112–118.
5. Patel BN, Gupta RT, Zani S, Jeffrey RB, Paulson EK, Nelson RC. How the radiologist can add value in the evaluation of the pre- and post-surgical pancreas. Abdom Imaging 2015;40(8):2932–2944.
6. Paik KY, Choi SH, Heo JS, Choi DW. Analysis of liver metastasis after resection for pancreatic ductal adenocarcinoma. World J Gastrointest Oncol 2012;4(5):109–114.
7. Driedger MR, Dixon E, Mohamed R, Sutherland FR, Bathe OF, Ball CG. The diagnostic pathway for solid pancreatic neoplasms: are we applying too many tests? J Surg Res 2015;199(1):39–43.
8. Park HS, Lee JM, Choi HK, Hong SH, Han JK, Choi BI. Preoperative evaluation of pancreatic cancer: comparison of gadolinium-enhanced dynamic MRI with MR cholangiopancreatography versus MDCT. J Magn Reson Imaging 2009;30(3):586–595.
9. Zhang Y, Huang J, Chen M, Jiao LR. Preoperative vascular evaluation with computed tomography and magnetic resonance imaging for pancreatic cancer: a meta-analysis. Pancreatology 2012;12(3):227–233.
10. Kim R, Prithviraj G, Kothari N, et al. PET/CT fusion scan prevents futile laparotomy in early stage pancreatic cancer. Clin Nucl Med 2015;40(11):e501–e505.
11. Rijkers AP, Valkema R, Duivenvoorden HJ, van Eijck CH. Usefulness of F-18-fluorodeoxyglucose positron emission tomography to confirm suspected pancreatic cancer: a meta-analysis. Eur J Surg Oncol 2014;40(7):794–804.
12. Farma JM, Santillan AA, Melis M, et al. PET/CT fusion scan enhances CT staging in patients with pancreatic neoplasms. Ann Surg Oncol 2008;15(9):2465–2471.
13. Shrikhande SV, Barreto SG, Goel M, Arya S. Multimodality imaging of pancreatic ductal adenocarcinoma: a review of the literature. HPB (Oxford) 2012;14(10):658–668.
14. Yoo HJ, Lee JS, Lee JM. Integrated whole body MR/PET: where are we? Korean J Radiol 2015;16(1):32–49.
15. Huellner MW, Appenzeller P, Kuhn FP, et al. Whole-body nonenhanced PET/MR versus PET/CT in the staging and restaging of cancers: preliminary observations. Radiology 2014;273(3):859–869.
16. Huellner MW, de Galiza Barbosa F, Husmann L, et al. TNM staging of non–small cell lung cancer: comparison of PET/MR and PET/CT. J Nucl Med 2016;57(1):21–26.
17. Catalano OA, Nicolai E, Rosen BR, et al. Comparison of CE-FDG-PET/CT with CE-FDG-PET/MR in the evaluation of osseous metastases in breast cancer patients. Br J Cancer 2015;112(9):1452–1460.
18. Drzezga A, Souvatzoglou M, Eiber M, et al. First clinical experience with integrated whole-body PET/MR: comparison to PET/CT in patients with oncologic diagnoses. J Nucl Med 2012;53(6):845–855.
19. Heusch P, Buchbender C, Köhler J, et al. Thoracic staging in lung cancer: prospective comparison of 18F-FDG PET/MR imaging and 18F-FDG PET/CT. J Nucl Med 2014;55(3):373–378.
20. Rauscher I, Eiber M, Fürst S, et al. PET/MR imaging in the detection and characterization of pulmonary lesions: technical and diagnostic evaluation in comparison to PET/CT. J Nucl Med 2014;55(5):724–729.
21. Nagamachi S, Nishii R, Wakamatsu H, et al. The usefulness of (18)F-FDG PET/MRI fusion image in diagnosing pancreatic tumor: comparison with (18)F-FDG PET/CT. Ann Nucl Med 2013;27(6):554–563.
22. Park MJ, Kim YK, Choi SY, Rhim H, Lee WJ, Choi D. Preoperative detection of small pancreatic carcinoma: value of adding diffusion-weighted imaging to conventional MR imaging for improving confidence level. Radiology 2014;273(2):433–443.

23. Katz MH, Crane CH, Varadhachary G. Management of borderline resectable pancreatic cancer. Semin Radiat Oncol 2014;24(2):105–112.

24. Ohno Y, Koyama H, Yoshikawa T, et al. N stage disease in patients with non–small cell lung cancer: efficacy of quantitative and qualitative assessment with STIR turbo spin-echo imaging, diffusion-weighted MR imaging, and fluorodeoxyglucose PET/CT. Radiology 2011;261(2):605–615.

25. Joo I, Lee JM, Kim JH, Shin CI, Han JK, Choi BI. Prospective comparison of 3T MRI with diffusion-weighted imaging and MDCT for the preoperative TNM staging of gastric cancer. J Magn Reson Imaging 2015;41(3):814–821.

26. Okada M, Murakami T, Kumano S, et al. Integrated FDG-PET/CT compared with intravenous contrast-enhanced CT for evaluation of metastatic regional lymph nodes in patients with resectable early stage esophageal cancer. Ann Nucl Med 2009;23(1):73–80.

27. Raman SP, Reddy S, Weiss MJ, et al. Impact of the time interval between MDCT imaging and surgery on the accuracy of identifying metastatic disease in patients with pancreatic cancer. AJR Am J Roentgenol 2015;204(1):W37–W42.

28. Heestand GM, Murphy JD, Lowy AM. Approach to patients with pancreatic cancer without detectable metastases. J Clin Oncol 2015;33(16):1770–1778.

29. Gangi S, Fletcher JG, Nathan MA, et al. Time interval between abnormalities seen on CT and the clinical diagnosis of pancreatic cancer: retrospective review of CT scans obtained before diagnosis. AJR Am J Roentgenol 2004;182(4):897–903.

30. Sergeant G, Ectors N, Fieuws S, Aerts R, Topal B. Prognostic relevance of extracapsular lymph node involvement in pancreatic ductal adenocarcinoma. Ann Surg Oncol 2009;16(11):3070–3079.

31. Padhani AR, Koh DM, Collins DJ. Whole-body diffusion-weighted MR imaging in cancer: current status and research directions. Radiology 2011;261(3):700–718.

32. Aljabery F, Lindblom G, Skoog S, et al. PET/CT versus conventional CT for detection of lymph node metastases in patients with locally advanced bladder cancer. BMC Urol 2015;15:87.

33. Holzapfel K, Reiser-Erkan C, Fingerle AA, et al. Comparison of diffusion-weighted MR imaging and multidetector-row CT in the detection of liver metastases in patients operated for pancreatic cancer. Abdom Imaging 2011;36(2):179–184.

34. Motosugi U, Ichikawa T, Morisaka H, et al. Detection of pancreatic carcinoma and liver metastases with gadoxetic acid–enhanced MR imaging: comparison with contrast-enhanced multi-detector row CT. Radiology 2011;260(2):446–453.

35. Queiroz MA, Kubik-Huch RA, Hauser N, et al. PET/MRI and PET/CT in advanced gynaecological tumours: initial experience and comparison. Eur Radiol 2015;25(8):2222–2230.

36. Michielsen K, Vergote I, Op de Beeck K, et al. Whole-body MRI with diffusion-weighted sequence for staging of patients with suspected ovarian cancer: a clinical feasibility study in comparison to CT and FDG-PET/CT. Eur Radiol 2014;24(4):889–901.

37. Lyons K, Seghers V, Sorensen JI, et al. Comparison of standardized uptake values in normal structures between PET/CT and PET/MRI in a tertiary pediatric hospital: a prospective study. AJR Am J Roentgenol 2015;205(5):1094–1101.

38. Jeong JH, Cho IH, Kong EJ, Chun KA. Evaluation of Dixon sequence on hybrid PET/MR compared with contrast-enhanced PET/CT for PET-positive lesions. Nucl Med Mol Imaging 2014;48(1):26–32.